Research Article

Thermal performance enhancement studies on a circular finned coil-in-shell heat exchanger using graphene oxide nanofluid

Niranjana Rai[1] · Ramakrishna N. Hegde[2]

Abstract
The objective of this study is to investigate the effect on heat transfer augmentation by the combined effect of circular fins directly attached to the helical surface of the coil in two different orientations (45° and 90°) and Graphene Oxide nanofluid as a heat transport agent, in a coil-in-shell heat exchanger. The attached circular fins not only act as turbulators on the shell side but could also add to heat transfer from the hot side to the cold side, by a combined mechanism of conduction and convection. The experiment is conducted at constant heat flux, with the cold nanofluid in the coil side and hot air in the shell side. Test runs are taken by varying hot air velocities from 1 m/s to 5 m/s, keeping fixed volume concentration of nanofluid (0.05–0.15%) and flow rate (500 ≤ Re ≤ 5500) one at a time. Experimental results indicated significant enhancement in heat transfer performance for the finned configuration. For 90° and 45° fin orientation—0.15% volume concentration of nanofluid, the maximum heat transfer increase is by 78.46%, and 82.22%, Nusselt number increase is by 32.57%, 60.79% respectively, at a hot air velocity of 3 m/s. The coil side pressure drop and friction factor increased to 32.72% and 24.64% for 0.15% GO nanofluid when compared to pure water at the maximum flow rate. The thermal–hydraulic performance improvement is nearly two-fold with 45° fin orientation-GO nanofluid combination.
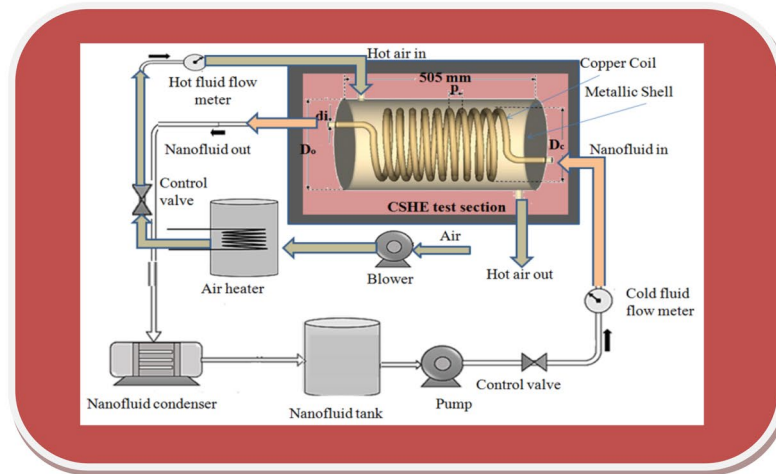
✉ Ramakrishna N. Hegde, rkhegderk@gmail.com; Niranjana Rai, niran4u@gmail.com | [1]Department of Mechanical Engineering, Canara Engineering College, Mangaluru, Karnataka 574219, India. [2]Department of Automobile Engineering, Srinivas Institute of Technology, Mangaluru, Karnataka 574143, India.
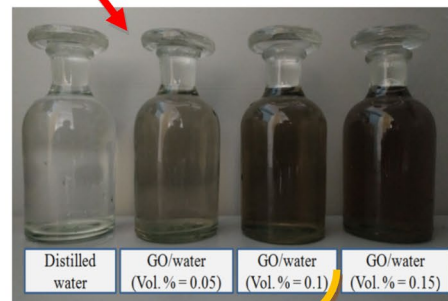
Graphic abstract
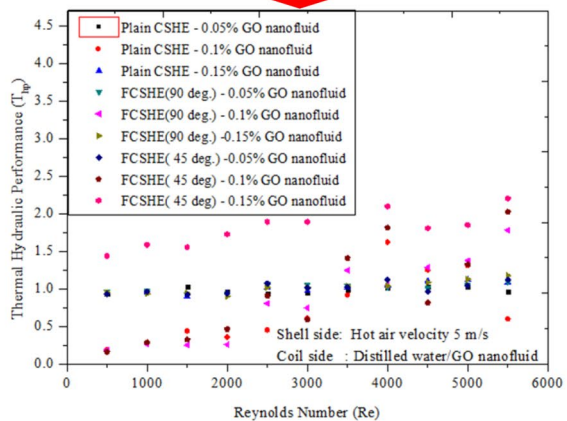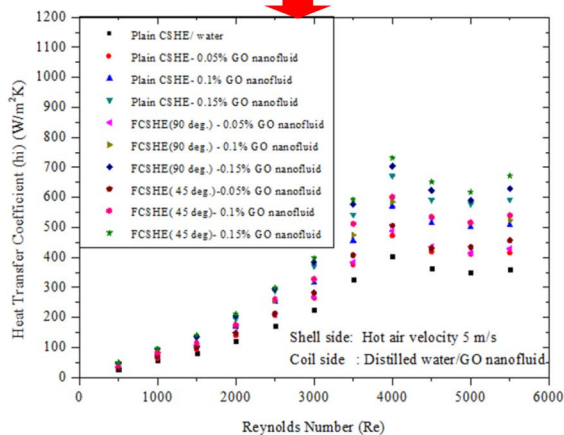
Abbreviations

CSHE	Coil in shell heat exchanger
CI	Confidence interval
FCSHE	Finned coil in shell heat exchanger
HAV	Hot air velocity
THP	Thermal hydraulic performance

Nomenclature

A_s	Effective surface area (m^2)
Cp	Specific heat of water (kJ/kg K)
D_c	Diameter of helical coil (m)
De	Dean number
D_{si}	Inner diameter of shell (m)
d_i	Inner diameter of coil tube (m)
f_c	Coil side friction factor
f_s	Shell side friction factor
h_i	Heat transfer coefficients (W/m^{2}K)
I	Current supplied (Ampere)
K	Thermal conductivity (W/m K)
L	Tube length (m)
L_s	Shell length (m)
M	Mass flow rate (kg/s)
N	Sample size
Nu	Nusselt number
P	Pitch of the coil (m)
q	Heat flux (W/m^2)
Q	Rate of heat transfer (kW)
Re	Reynolds number
T	Temperature (K)
T_{hp}	Thermal hydraulic performance
V	Voltage (V)
V_{ha}	Hot air velocity (m/s)
$\bar{X}$	Sample mean
Z	1.96 (CL = 95%)

Greek/Roman symbols

ρ	Density (kg/m^3)
μ	Absolute viscosity (Ns/m^2)
φ	Volume concentrations of nanofluids (%)
δ	Curvature ratio
α	Fin orientation
σ	Standard deviation

Subscripts

bf	Base fluid
c	Coil
ci	Cold fluid inlet
co	Cold fluid outlet
h	Hot fluid
hi	Hot fluid outlet
ho	Hot fluid outlet
f	Base fluid
nf	Nanofluid
p	Particle
s	Surface

1 Introduction

The augmentation of heat transfer facilitates a significant reduction in the size of heat exchangers. Using coil-in-shell heat exchanger (CSHE) instead of straight pipes offers higher heat transfer rate, improved pressure drop, compactness, a secondary flow to boost the turbulence as well as delays in the annular flow regime. Besides, it finds a wide range of applications viz., in steam, gas, nuclear power plants, in HAVC systems, in dairy and food processing industries, etc [1, 2]. Using effective intensification methods like active, passive, and combined techniques, enhancement of heat exchanger performance by optimizing pumping power can be achieved. Heat transfer augmentation in active technique requires an external power source, which leads to an increase in the overall cost. Conversely, the passive method involves some enhancement techniques like geometrical variations, insertion of different geometrical shapes, extended surfaces like fins, the addition of nanoparticles to the heat-carrying fluid, etc [3–5]. Many investigators follow a line of investigation to improve the heat exchanger performance by using several passive augmentation approaches in coil-in-shell heat exchangers (CSHE). Such an extensive study appropriate to the present investigation are summarized hereunder.

Many investigators follow a line of investigation that improves heat exchanger performance. Lin and Ebadian [6] studied the Nusselt number (Nu) is a wholly developed thermal section of helical pipes. The authors stated that local average Nu fluctuates before becoming steady in thermally fully developed section, specifically for large curvature ratios. Jayakumar et al. [7] reported that the influence of pitch of the helical coil on a fully developed Nu number was relatively less significant in the studied range. Babita et al. [8] experimented on the helical coil heat exchanger for various curvature ratio (0.036–0.067) at different volume concentration of CNT nanofluid (0–0.051%) under the laminar regime. The authors reported a rise in friction factor with the increase in the curvature ratio and volume concentration of nanofluid.

Jamshidi et al. [9] studied the flow characteristics by varying the coil diameter and pitch ($0.0813 < D_c < 0.116$, $13 < P_c < 18$) with pure water as working fluid, under laminar flow regime. They depicted the improvement in heat transfer rate with the higher coil diameter, coil pitch, and mass flow rate in the shell and tube. Omidi et al. [10] reported the influence of small tube diameter in the helical tube heat exchanger on the Nu and friction factor. They

found that Nu was increasing as volume concentration of Al_2O_3 nanofluid increased and observed a higher value of Nu, compared to base fluid with minimum pumping power. Steady-state turbulent forced convection flow of CuO nanofluid inside helically coiled tubes at constant wall surface temperature was investigated through analytical and experimental techniques by Rakhsha et al. [11]. The analytical results revealed 6–7% and 9–10% improvement in heat transfer and pressure loss, respectively. In comparison, the experimental results indicated the enhancement of 16–17% and 14–16%, respectively, for different tube geometries at various Reynolds numbers (Re). Ghorbani et al. [12] conducted experiments on mixed convection heat transfer in a helical-coiled shell heat exchanger in a vertical position. They found that the axial temperature of the heat exchanger was beneficial for the ratio of the mass flow rate of the tube-side to the shell-side. Akhavan-Behabadi et al. [13] investigated heat transfer enhancement in vertical helically coiled tubes using nanofluid in the thermal entrance region. They found that helically coiled tubes improve the heat transfer rate extensively compared to the straight tube.

Khosravi-Bizhaem and Abbassi [14] conducted a numerical study on the effects of Al_2O_3/water nanofluid in a helical coil on heat transfer improvement in the laminar flow regime. They demonstrated higher heat transfer for the higher curvature ratios. Boonsri and Wongwises [15] studied the performance of a copper helical-coiled and aluminum crimped, spiral, finned-tube heat exchanger subjected to hot water and ambient air combination as working fluids. The test runs were done at air mass flow rates in the range of 0.04–0.13 kg/s and water mass flow rates of 0.2–0.4 kg/s. The water temperatures were between 40 °C and 50 °C. The study revealed that the projected mathematical model could simulate the experimental data comparatively fit, in particular, at higher air velocity. Water mass flow rate and the inlet water temperature had significant effects on the outlet air and water temperatures. The outlet air and water temperatures reduced with the rising air velocity. Sadeghzadeh et al. [16] designed and optimized a finned shell and tube heat exchanger using a multi-objective genetic algorithm for maximization heat transfer and minimize the cost. The authors illustrated the Pareto curve for optimization by considering variables like arrangement of the tube, tube pitch ratio, number of tubes, tube length, tube diameter, fin height, fin thickness, number of fins per unit length, and baffle spacing ratio. Andrzejczyk et al. [17] experimentally studied the effect of variable baffles geometry and its orientation (45°) on augmentation of heat transfer in shell coil heat exchanger. They suggested using the turbulators at the shell side. They observed considerable raise in heat transfer in the laminar regime for optimal baffle configuration. Nada et al. [18] experimentally studied dehumidifying helical coils with strips fins at horizontal and vertical positions for various flow rates of air. They affirmed that strip fins enhance the performance of the coil in both orientations for all studied range of airflow. Rajesh Kumar et al. [19] experimentally investigated that finned helical coil heat exchanger exhibits heat transfer coefficient 15–16% higher than an un-finned heat exchanger. They also observed a drop in temperature with an increased flow rate of hot water in the test section.

From the detailed literature review, it can be concluded that nanofluids and finned turbulators can be used as the two different passive methods to improve the thermal performance of a coil-in-shell heat exchanger (CSHE). Besides, there have been studies on the combined augmentation technique using nanofluid as cold fluid flowing through an open helical coil with different geometrically configured turbulator inserts within the helical loop on the shell-side in a CSHE. There is no available literature where a combined technique using Graphene Oxide nanofluid and directly mounted circular fins on the helically coiled surface is used. The objective of this study is to investigate the effect on heat transfer augmentation by attaching the circular fins directly on the helical surface of the coil itself in two different orientations (45° and 90°), while nanofluid is acting as a cold fluid. The attached circular fins not only act as turbulators on the shell side but could also add to possible heat transfer from the hot side to the cold side, by a combined mechanism of conduction and convection. The effect of the finned coil arrangement on the overall thermal performance of coil-in-shell heat exchanger, in different volume concentrations of Graphene oxide nanofluid (cold fluid) at different flow rates of hot air (hot fluid), is the research focus of this study.

The structure of the current paper is organized into five major sections. Section 1 focuses on the current state of research in the field of heat exchangers supplemented by a literature survey, the gap in the research, and the relevance of the present investigation to bridge the research gap. Section 2 explains the preparation of nanofluids and its properties. Section 3 discusses experimental details, namely about the experimental setup, experimental

Table 1 Physical properties of GO nanofluid (as per data provided by the manufacturer)

Chemical formula	Color	Oxygen content	Morphology	pH	Residue on evaporation	Partial size
$C_{2.19}H_{0.8}O_{1.00}$	Dark brown	42%	Monolayer Graphite flake	2.1	3.8	45 nm

(a)   (b)
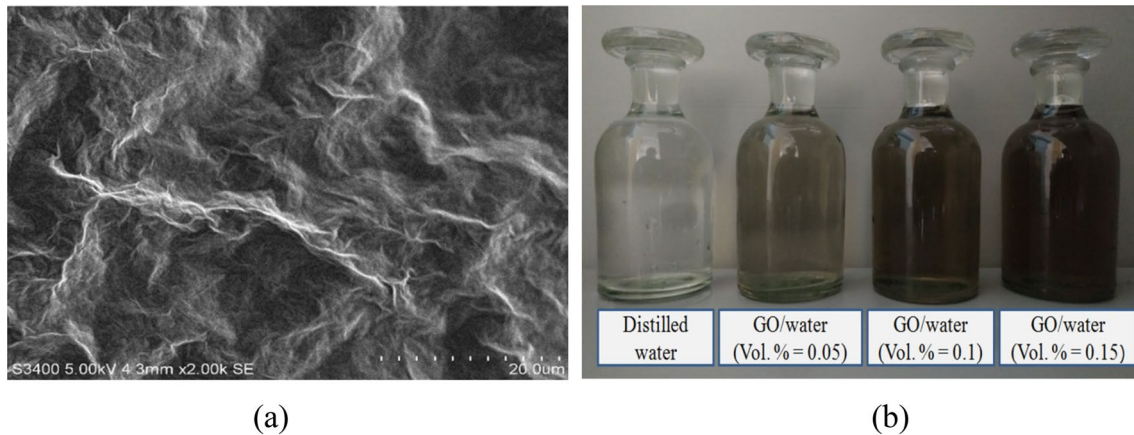
Fig. 1 **a** SEM image of dispersed GO/water nanofluid, **b** GO-water nanofluid

procedure, experimental uncertainty, and data reductions. Section 4 is dedicated to explaining the results along with a discussion on experimental validation, performance characteristics, like average Nusselt number, friction factor, and Thermal Hydraulic Performance (THP) for both normal and finned configurations. The work is summarized and concluded in Sect. 5.

2 Preparation of nanofluid and its properties

Graphene-water nanofluid with a concentration of 4 mg/ml nanoparticles suspended in the fluid was in the range of 20–50 nm. It was procured from Sigma-Aldrich®, USA. The fluid volume concentrations were considered in the study were 0.05%, 0.1%, and 0.15% of GO nanofluid through dispersed GO in the base fluid (distilled water) as mentioned elsewhere [20, 21]. The nanofluid was stirred in a high-speed stirrer (3000 rpm) for 2 h before experimenting. Poly-vinyl-pyrrolidone (PVP) was used as a surfactant to ensure the stabilization of nanofluid. Figure 1a shows the SEM image of GO nanoparticles' average size of particles used was 45 nm as tested using a Particle Size Analyzer. The 'thicker' and 'multi-layer' looking GO sheets could be attributed to the existence of covalently bound oxygen and sp^3 hybridized carbon atoms located near to the original Graphene plane [22]. Figure 1b shows GO/water nanofluid at different volume concentrations used for the experimental investigations. The physical properties of GO nanofluid are presented in Table 1. The thermophysical properties of GO nanofluid are found at various temperatures for various volume concentrations (0.05%, to 0.15%) based on correlations available in the literature [11, 23]

The density of nanofluid in kg/m³;

$$\rho_{nf} = \phi\rho_p + (1 - \phi)\rho_{bf} \tag{1}$$

Dynamic viscosity in N-s/m²;

$$\mu_{nf} = \mu_{bf}(1 + 2.5\phi) \tag{2}$$

Specific heat in J/kg-K;

$$C_{nf} = \phi C_p + (1 - \phi)C_{bf} \tag{3}$$

Thermal conductivity in W/m–K;

$$k_{nf} = \left[\frac{K_p + 2K_{bf} + \phi 2(K_p + K_{bf})}{K_p + 2K_{bf} + \phi(K_p + K_{bf})} \right] \tag{4}$$

3 Experimental details

The details of the experiment are discussed considering experimental test rig, the procedure followed for experimentation, the uncertainty of the measuring devices, and equations used for achieving the results.

3.1 Experimental set up

The schematic layout of the experimental setup shown in Fig. 2a consists of two loops viz., shell region loop, and helically coiled region loop. Shell region loop handles hot air, and the coiled tube loop handles GO nanofluid, in counterflow condition.

The experimental setup consists of a test section, an air heater (0–1500 W), a centrifugal blower (1.5 kW), a centrifugal pump, nanofluid collecting tank, a condenser, a power meter (0–4.5 kW), a rotameter (0–4 lpm), an anemometer (0–15 m/s), and K-type thermocouples (0–100℃). A set of K-type thermocouples (10 numbers) is attached to

Fig. 2 **a** Schematic layout of CSHE test rig, **b** schematic view FCSHE test section

(a)

(b)
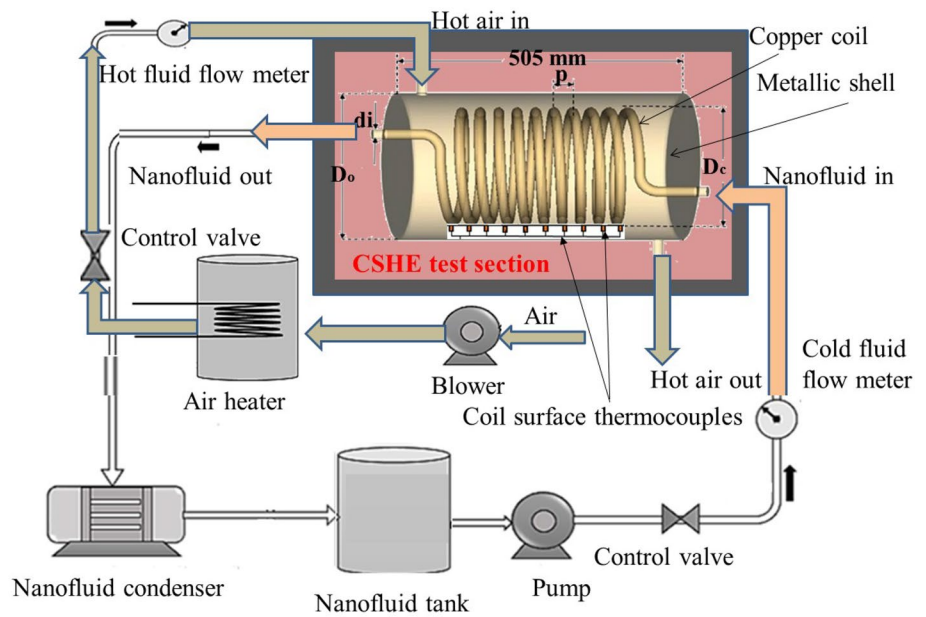
Fig. 3 Plain and finned configurations of coil

Plain coil   90°- Orientation coil   45° - Orientation coil

the coil surface at equal distance to measure the average surface temperature of the test section. Figure 2b shows

the test section of a copper tube of 0.010 m inner diameter and 0.013 m outer diameter wound in helical shape

Table 2 Uncertainty of measuring devices

Measuring device	Range	Uncertainty (%)	Resolution
Rota meter	0–4 lpm	±0.02	0.01 lpm
K-type thermocouple	0–100 °C	±0.01	0.01 °C
Anemometer	0–15 m/s	±0.01	0.01 m/s
Voltmeter	0–300 V	±0.03	0.1 V
Ammeter	0–50 A	±0.02	0.01A
Pressure gauges	0–1 mbar	±0.01	0.001 mbar

with curvature ratio (δ) of 0.142 and pitch of 0.014 m, surrounded with a shell of 0.116 m inner diameter, made up of stainless steel with thickness 0.003 m. The coil 8.5 m long with 36 turns. The total length of the test section is 0.505 m.

Three helical coils, comprising two with circular fins attached to the surface of the coil and other without circular fins, were used for the study. The circular copper fin brazed at 90° and 45° over the surface of the helical coil, as shown in Fig. 3. The dimensions of circular fin viz., diameter 0.004 m, and length 0.010 m with fin ratio $\Psi = 0.4$.

3.2 Experimental procedure

The experiment is conducted by varying flow rates of cold fluid ($500 \leq Re \leq 5500$) in the coil side loop and hot air velocity (HAV) from 1 m/s to 5 m/s ($4500 \leq Re \leq 22{,}500$) in the shell side loop at a constant heat flux of 4 kW/m². The initial run is taken with pure distilled water-hot air combination, for both CSHE and FCSHE (90° and 45° orientation) configurations. Whereas for the subsequent run, distilled water is replaced with Graphene oxide (GO) nanofluid with varying volume concentrations of 0.05%, 0.10%, and 0.15%, the other test parameters being kept constant.

3.3 Experimental uncertainty

In the present study, the uncertainty of obtained results is vital as it ensures the legitimacy of the measured and presented experimental values. The uncertainty of any measured data is projected based on the normal distribution method with confidence limits of $\pm 2\sigma$ (95.45% of the measured data recline within the edge of $\pm 2\sigma$ of the mean). Thus, the uncertainty of any measured parameter is given by [24],

$$CI = \bar{X} \pm Z\left(\frac{\sigma}{\sqrt{n}}\right) \qquad (5)$$

Experiments were employed to obtain the confidence interval (CI) and standard deviation (σ) of Nu and friction factor. The analysis was done for three sets of readings under the same operating conditions for the base fluid combination. The margin error lies within ± 0.526 of mean for Nu and ± 0.0018 of the mean for friction factor, while error for standard deviation obtained was 0.379 and 0.0013, respectively. The uncertainty in measuring devices [24] is presented in Table 2 below.

The maximum uncertainties of derived quantities are 1.02% for Reynolds number, 1.12% for heat transfer coefficient, 1.91% for Nusselt number, 1.01% for friction factor, and 1.18% for thermal hydraulic performance respectively. The overall experimental uncertainty is 2.44%.

3.4 Data reduction

For constant heat flux and variable flow velocity of hot air (1–5 m/s), based on experimental observation, for different studied combinations under steady state condition, the Logarithmic Mean Temperature difference (LMTD), heat transfer coefficient, Nusselt number and the friction factor of the heat exchanger were calculated using Eqs. (6)–(13) [1, 7, 15].

- The heat transfer (Q) for hot air and GO/water nanofluid (Heat gained);

$$Q = m_h C_{ph}(T_{hi} - T_{ho}) = m_c C_{pc}(T_{co} - T_{ci}) \qquad (6)$$

- Average heat transfer (Q_{avg});

$$Q_{avg} = \frac{(Q_h + Q_c)}{2} \qquad (7)$$

- The surface temperature of the coil (T_s);

$$T_s = \frac{(T_1 + T_2 + \cdots + T_{10})}{10} \qquad (8)$$

- Bulk temperature of Cold fluid (T_{Bc});

$$T_{Bc} = \frac{T_{ci} + T_{co}}{2} \qquad (9)$$

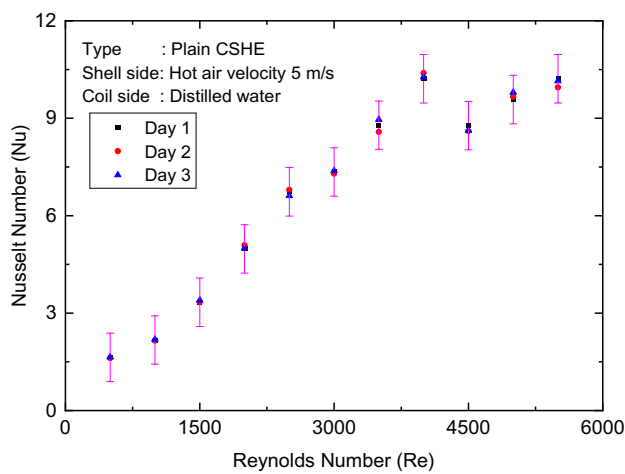- LMTD for the counter flow array is;

$$LMTD = \frac{(T_{hi} - T_{co}) - (T_{ho} - T_{ci})}{\ln\left[\frac{(T_{hi}-T_{co})}{(T_{ho}-T_{ci})}\right]} \qquad (10)$$
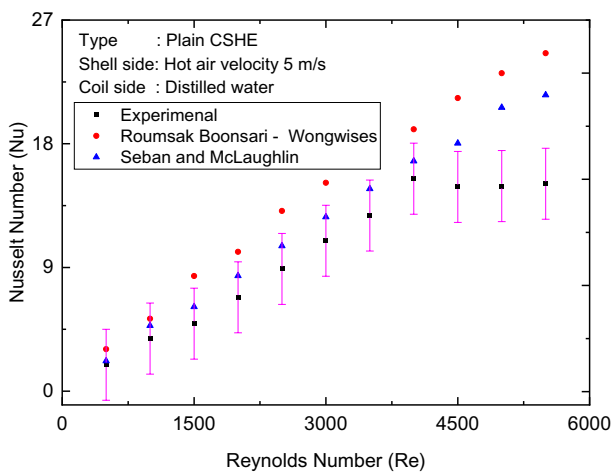
- Heat transfer coefficient (h);

$$h = \frac{Q}{A(T_S - T_{Bc})} \qquad (11)$$
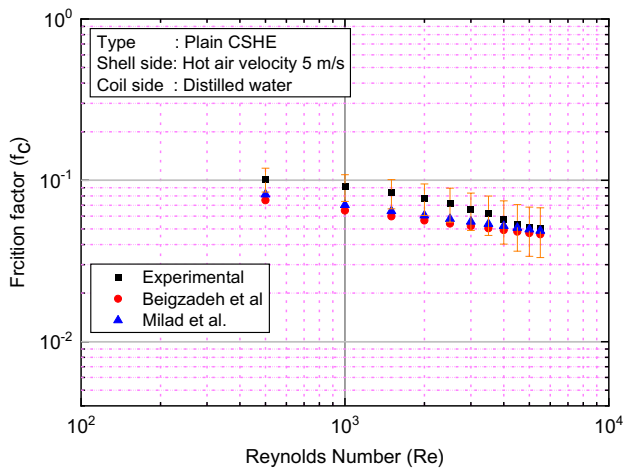
- Coil side friction factor (f_c);

$$f_c = 0.046 Re^{-0.2}[De]^{\frac{1}{20}} \qquad (12)$$

(a)

(b)

(c)

Fig. 4 **a** Nu v/s Re for repeatability, **b** coil side Nu with the past works for validation [15, 26], **c** friction factor v/s Re for validation [11, 27]

- Shell side friction factor (f_s);

$$f_s = \frac{2\Delta p D_{si}}{0.0689476 \rho L_s (V_{ha})^2} \tag{13}$$

- Key dimensionless parameters viz., Re, Pr, Nu and Dean Number (De) were calculated using Eqs. (14)-(17) [25].
- Reynolds Number,

$$Re = \frac{\rho V d_i}{\mu} \tag{14}$$

- Prandtl Number,

$$Pr = \frac{\mu C_p}{k} \tag{15}$$

- Nusselt Number,

$$Nu = \frac{h d_i}{k} \tag{16}$$

- Dean Number,

$$De = Re \left(\frac{d_i}{D_c} \right)^{1/2} \tag{17}$$

## 4 Results and discussion

4.1 Repeatability and validation

Figure 4a indicates repeatability of experiment comprising the data taken on three different days under same working condition for the plain CSHE with shell side at HAV 5 m/s (Re = 22,500) and distilled water on coil side at $500 \leq Re \leq 5500$. The obtained deviation lies within ± 0.24% to ± 1.53% with standard deviation. Experimental Nu and friction factor results of fully developed laminar to turbulent flow region in CSHE were confirmed by comparing with existing correlations respectively by Seban and McLaughlin [26], Boonsri et al. [15] and Beigdzadeh et al. [27], Milad et al. [11] as illustrated in Fig. 4b and c. It can be observed that experimental Nu and friction factor deviations were ± 4.54% and ± 0.0179% respectively from the theoretical values.

Referring Fig. 4b, the deviation of Nu at Re > 4000 could be due to the higher turbulence and consequent lower resident time available to extract the heat from the coil surface effectively. This will affect the overall heat transfer from the coil surface to cold fluid, reducing the experimental Nu. The deviation of experimental Nu with existing correlation could be attributed to the coil material, experimental uncertainty, different trial conditions, range of parameters, and intrinsic losses in the test set rig, etc.
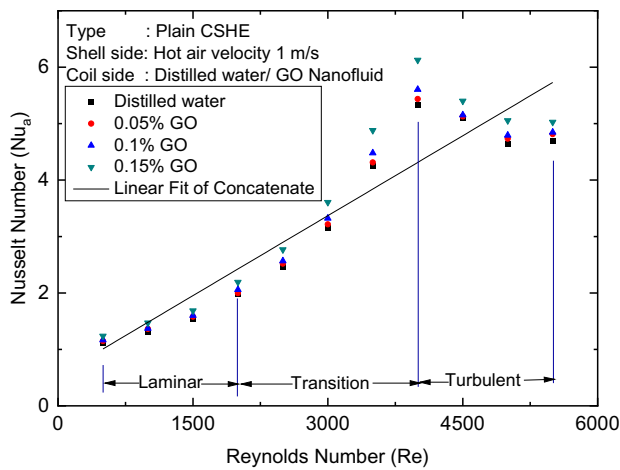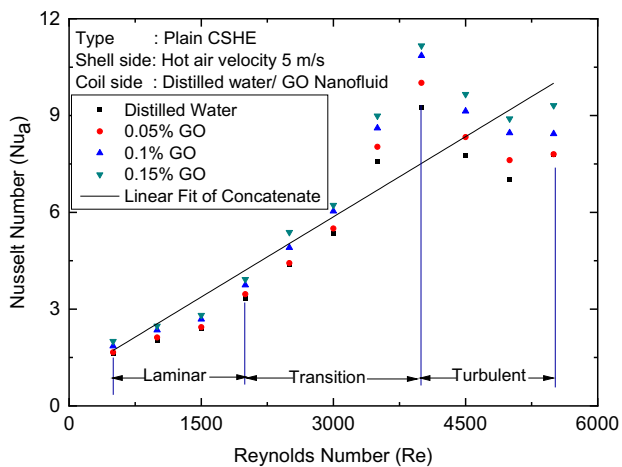
(a) CSHE with HAV=1 m/s
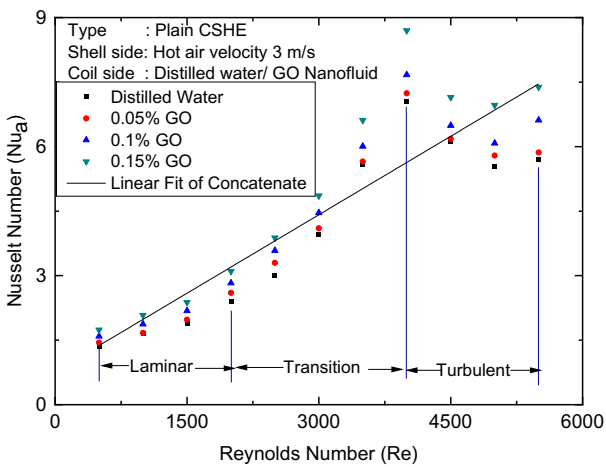
(b) CSHE with HAV = 3 m/s

(c) CSHE with HAV = 5 m/s

Fig. 5 Average Nu v/s Re in different volume concentrations of GO at different HAVs in CSHE
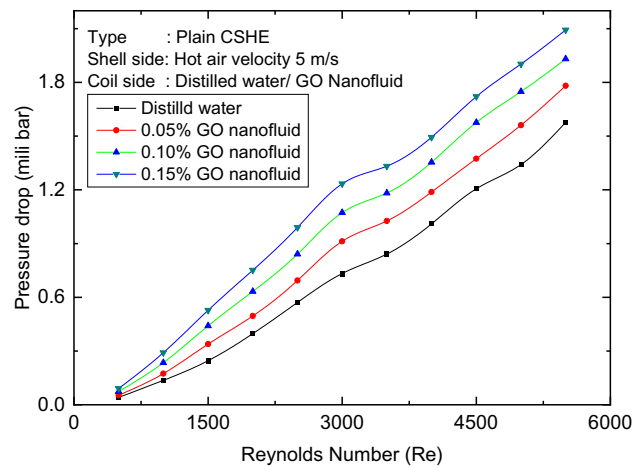

Fig. 6 Coil side pressure drop with Re for GO/water nanofluid in CSHE
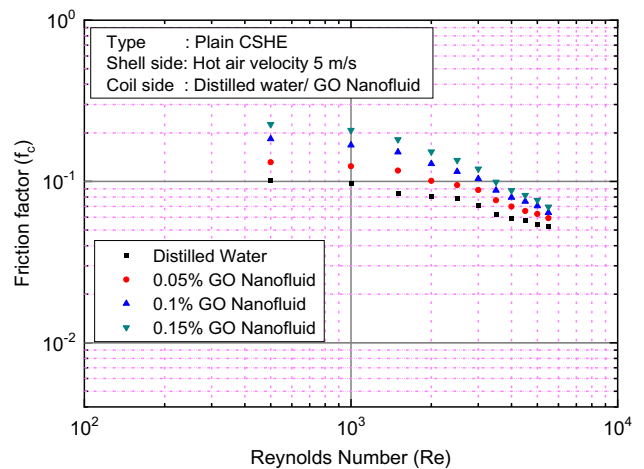

Fig. 7 Coil side friction factor with Re for GO/water nanofluid in CSHE

4.2 Performance characteristics of the plain CSHE

4.2.1 Effect on Nusselt number

Figure 5 illustrates the variation of average Nu (Nu_a) with Re at different HAVs (1–5 m/s) and volume concentrations of GO/water nanofluid (0.05–0.15%) for plain CSHE. The average Nu increased with HAV for all volume concentrations of nanofluid both in laminar and turbulent flow regimes. The average Nu increased to 7.12% in 0.15% volume concentration of GO nanofluid at Re = 5500 compared to distilled water at HAV = 1 m/s (Fig. 10 a). Besides, it was increased to 19.49% for the same flow conditions of cold fluid compared to distilled water at HAV = 5 m/s (Fig. 5c). The maximum enhancement recorded was 29.47% at
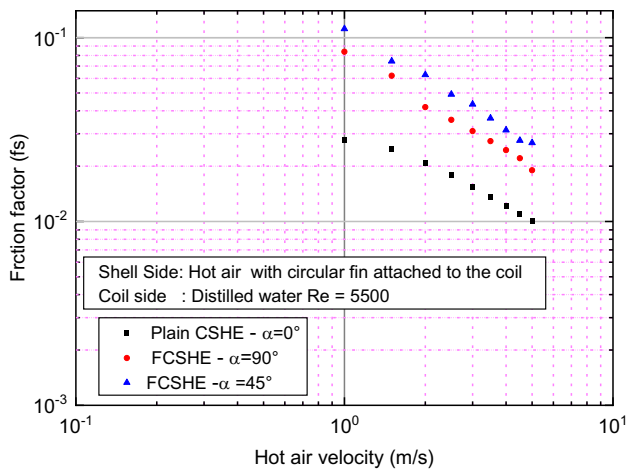
**Fig. 8** Shell side friction factor with HAV in FCSHE

HAV = 3 m/s (Fig. 5b). One of the reasons for the enhancement in Nu could be due to the presence of GO nanoparticle in base fluid results in increased thermal conductivity. Many theories explain the mechanism behind the improvements in thermal conductivity of nanofluid, for instance, the theory of ballistic heat transports and liquid layer, the theory of percolation, the theory of Brownian motion, and micro convection theory. Besides, numerous factors are influencing the augmentation of thermal conductivity of GO nanofluid, such as volume concentration, size of GO particle, preparation of nanofluids, type of graphite, and mass flow rate of nanofluid. These factors are believed to create turbulence in nanoparticles (small-sized nanosheets) motion resulting in micro-convection, which dominates, and hence, the thermal conductivity increases with increasing the temperature. Thus, GO nanofluid acts as a heat carrier and absorbs heat near the hot surface of the coil. Subsequently, this heat is carried to the cold side of the water (base fluid) [28, 30].

### 4.2.2 Effect on pressure drop and friction factor

Figures 6 and 7 respectively show the variation of pressure drop and friction factor with Re when HAV was maximum (5 m/s). For volume concentration of 0.15% GO nanofluid, the pressure drop was approximately 47.92% higher at Re = 4000 and 32.72% higher at Re = 5500 when compared with pure water. The friction factor increased to 121.94% at Re = 500 and by 24.64% at Re = 5500. The increase could be attributed to the presence of nanoparticles [29, 30, 31], changing the degree of turbulence and curvature ratio, the intensity of the secondary flow [11, 31]. Since a higher mass flow rate drastically reduces the friction factor, it is beneficial to use the GO/water nanofluid in the turbulent region with a small penalty in pumping power.
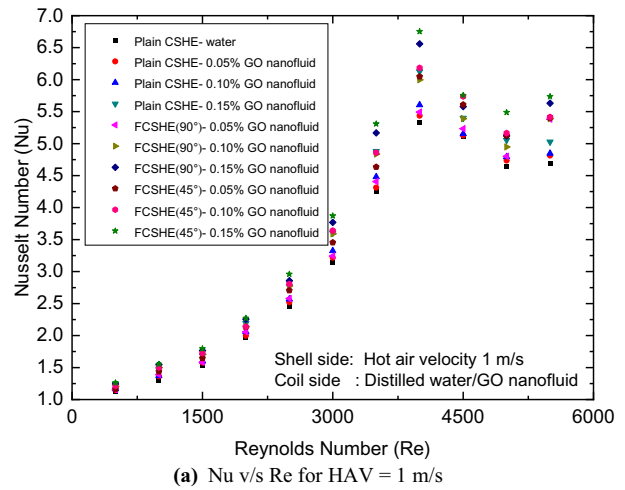
(a) Nu v/s Re for HAV = 1 m/s
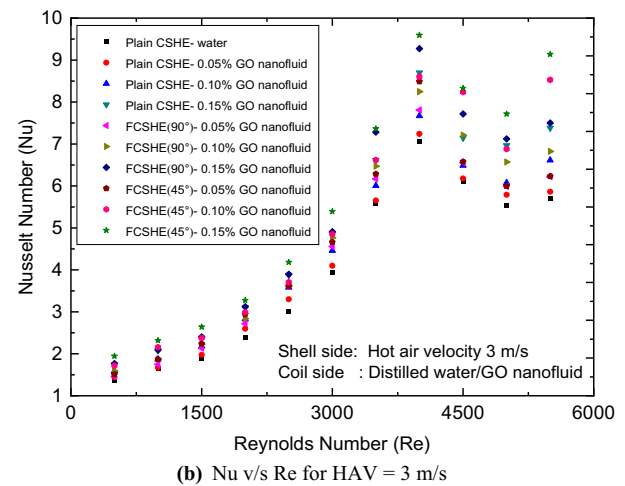
(b) Nu v/s Re for HAV = 3 m/s
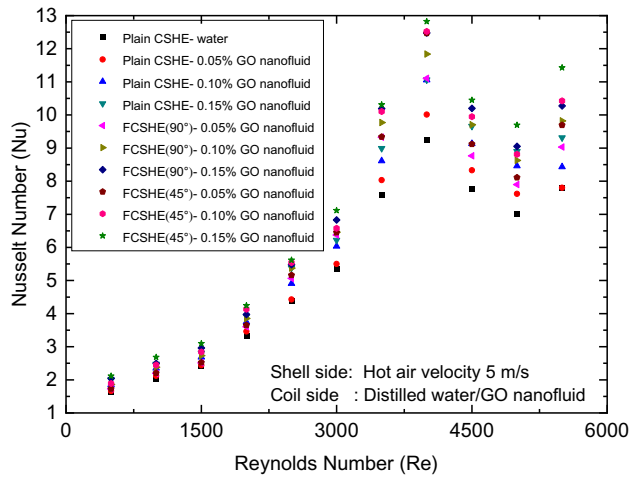
(c) Nu v/s Re for HAV= 5 m/s

Fig. 9 Nusselt number v/s Reynolds number at different HAVs for CSHE and FCSHE

Table 3 Nu enhancement with CSHE and FCSHE for 0.15% GO nanofluid compared to CSHE in pure water

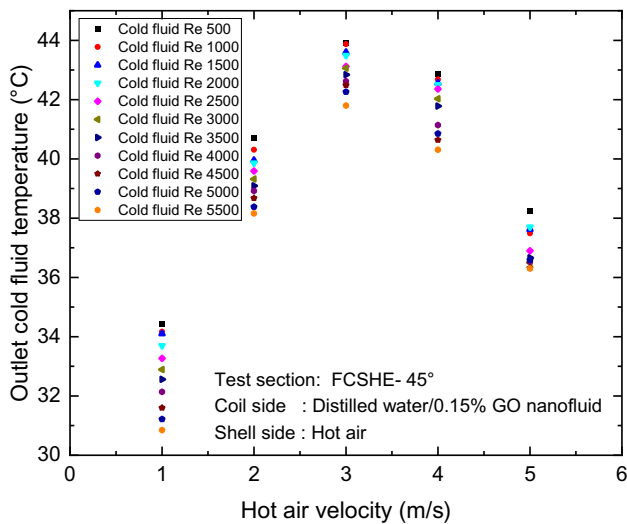| Working fluid	HAV (m/s)		
	1	3	5
0.15%GO nanofluid-CSHE	6.5%	29.30%	19.51%
0.15%GO nanofluid-FCSHE-90°	20.04%	32.57%	31.83%
0.15%GOnanofluid-FCSHE-45°	22.17%	60.01%	46.59%

Fig. 10 Variation of the outlet temperature of cold fluid with HAV for FCSHE-45°–0.15% GO nanofluid combination

Figure 8 shows the variation of shell side friction factor with hot air velocity with the finned configuration. The shell side friction factor increases for FCSHE as compared to plain CSHE. The reasons could be attributed to various factors like restrictions of flow conduit, generation of the eddy, higher surface contact area, turbulent flow, and pressure drop of the air due to high viscosity loss near shell wall. Further, the possibility of interaction of pressure forces with inertia forces in the boundary [31] could also result in pressure drop.

4.3 Synergistic effects of fin and GO nanofluid

The performance of FCSHE is compared with CSHE based on the Nu, outlet temperatures of nanofluid and thermal–hydraulic performance. It is observed that heat transfer enhanced in the turbulent region, i.e., at Re > 4000, for all configurations of the fin geometry and volume concentrations of nanofluid.

4.3.1 Effect on Nusselt number

Figure 9 shows the performance comparison of CSHE and FCSHE at different volume concentrations of GO nanofluid at different HAVs of 1–5 m/s. It is evident that FCSHE shows better performance with both the finned orientations. A comparative performance based on Nu for both CSHE and FCSHE configurations, with 0.15% of the volume of GO nanofluid, is given in Table 3. It may be observed that the percentage enhancement in Nu decreased at higher HAV = 5 m/s. The decrease in Nusselt number enhancement and the outlet water temperature was found to be having a direct bearing on the effective surface temperature of the finned coil at different HAVs. At HAV = 1 m/s, the effective surface temperature of the was 32.52 °C, which reached a maximum of 42.82 °C at HAV = 3 m/s.

Further increase in hot air velocity (HAV = 5 m/s) resulted in a drop in effective temperature, to 36.77 °C. This trend not reported earlier works of literature, and it is evident that if the fins are mounted directly on the surface of the helical coil, there is an optimum value of HAV at which the heat transfer enhancement is maximum. In the present work, the maximum percentage enhancement reaches when HAV = 3 m/s and then reduces at a higher value of HAVs, as seen in Fig. 10. The reason for the drop in effective surface temperature could be attributed to a shorter residence time of hot air molecules owing to increased turbulence [27] coupled with losses due to friction, eddy formation, etc. With the finned configuration, at lower hot air velocity (HAV = 1 m/s in this case), the mass flow rate of hot air is lower, and the resulting turbulence is also lower. The flow has lower frictional losses, as evident in Fig. 8. Though the residence time of air molecules is higher, the heat transfer rate is less from the shell side due to minimum turbulence.

On the other hand, at higher hot air velocity, the rate of heat transfer increases, consequently increasing the exergy loss. As per the available literature, the rate of heat transfer between two fluids with different temperatures always destroys the energy [32].

Another factor to be considered here is the synergetic effect of nanofluid and the increased heat transfer surface area. While nanofluid is a better heat transport agent, each fin added increases the area of the contact surface. The FCSHE-45°fin orientation enabled mounting of more number of fins on the coil, which resulted in higher surface area of contact. Hence the heat transfer enhancement is higher for FCSHE-45° orientation –0.15% GO nanofluid combination as compared to CSHE—distilled water combination for all HAVs. Since FCSHE 45° fin orientation enabled mounting of more number of fins on the coil surface than FCSHE 90°, the resulting surface area of contact to hot air was higher. The higher surface area enabled higher exergy
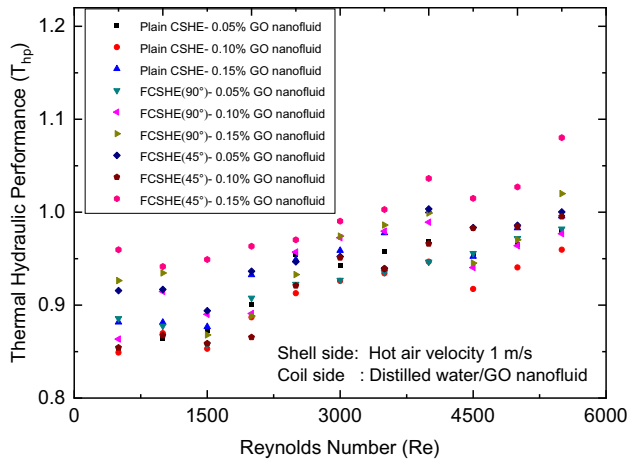
(a) THP v/s Re at HAV = 1 m/s
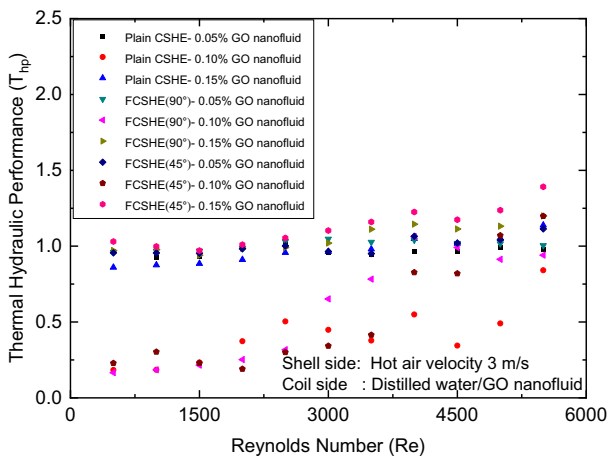
(b) THP v/s Re at HAV = 3 m/s
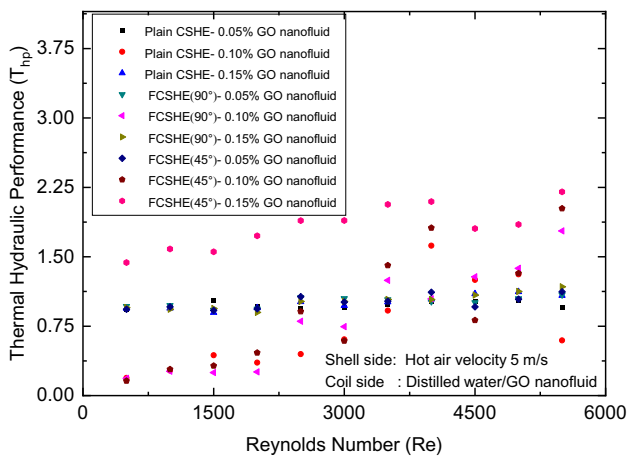
(c) THP v/s Re at HAV = 5 m/s

Fig. 11 Thermal hydraulic performances of CSHE and FCSHE

Table 4 Enhancement of heat transfer coefficient (h_i) with CSHE and FCSHE at 0.15% GO nanofluid compared to CSHE in pure water

Working fluid	HAV (m/s)		
	1	3	5
0.15%GO nanofluid-CSHE	40.51%	64.54%	64.13%
0.15%GO nanofluid-FCSHE-90°	42.25%	78.46%	74.48%
0.15%GOnanofluid-FCSHE-45°	44.02%	82.22%	80.70%

Table 5 Enhancement of THP with CSHE and FCSHE at 0.15% GO nanofluid compared to CSHE in 0.05% GO nanofluid

Working fluid	HAV (m/s)		
	1	3	5
0.15% GO nanofluid-CSHE	1.73%	16.08%	19.08%
0.15% GO nanofluid-FCSHE-90°	4.19%	22.26%	28.98%
0.15% GOnanofluid-FCSHE-45°	10.34%	41.92%	56.47%

(available heat) loss from shell-side fluid to coil side fluid [33–35]. Thus it can be concluded that the synergetic effect of the nanofluid and circular fin with proper orientation will enhance the rate of heat transfer. Hence for better heat transfer performance of heat recovery systems, FCHE 45° orientation with 0.15% GO nanofluid combination at HAV 3 m/s could be suitable.

The comparative performance in terms of the heat transfer coefficient for both CSHE and FCSHE configurations using 0.15% of the volume of GO nanofluid is given in Table 4.

4.3.2 Effect on THP

To estimate the thermodynamic gain such as the effectiveness of FCSHE over CSHE the experimental results in terms of performance assessment criterion can be analyzed and presented in terms of THP as per the Eq. 18 [2, 31].

$$T_{hp} = \left[\frac{\frac{Nu_p}{Nu_w}}{\frac{f_p}{f_w}} \right] \times (\delta)^{0.003} \qquad (18)$$

Figure 11 illustrates the influence of studied parameters on THP performance of heat exchanger. The performance index is high for FCSHE-45° orientation at 0.15% GO nanofluid combination. The maximum value of THP is 2.24, under turbulent regime at Re = 5500, for HAV = 5 m/s, 50.90% higher than that for HAV = 1 m/s (refer Fig. 11a, c) and 36.8% higher than at HAV = 3 m/s (refer Fig. 11b). Furthermore, when compared to FCSHE-90° orientation, the performance is 46.81% better under the same flow conditions (HAV = 5 m/s) and volume concentration of nanofluid.

Table 5 shows the relative enhancement of THP with CSHE and FCSHE at 0.15% GO nanofluid compared to CSHE in 0.05% GO nanofluid. The TPH increased with increased Re and volume concentrations of nanofluid. It is greater than unity for both configurations of FCSHE in the turbulent regime. The THP defined by Eq. (18) is a function of the Nusselt number and friction factor. While the fin orientation influences the Nusselt number, the volume concentration of nanofluid, and HAV, the friction factor is influenced by fin orientation and volume concentration of nanofluid. As a result of this for HAV = 5 m/s and 0.15% GO nanofluid for FCSHE-45°, the friction factor is less compared to HAV = 3 m/s for the same operating condition. Besides, the friction factor of the base fluid is less than that of nanofluids. Due to this, although the value of Nu is higher, the overall value of the THP increases.

5 Conclusion

An experimental investigation was done to study the thermal performance of a coil in a shell heat exchanger. The effect of circular fins mounted directly on the helical coil surface at two different orientations (45° and 90°) in conjunction with GO-water nanofluid on the heat transfer augmentation was studied. The experiments were conducted from laminar to a turbulent region (Re = 500–5500) under constant heat flux with different concentrations of nanofluids (0.05–0.15%) at the coil side and for different HAVs (1 m/s to 5 m/s) at shell side. The investigation revealed that the fin mounted helically coiled surface could not only disturb the hot fluid flow but also assist in and enhance the heat transfer. There is an optimum hot fluid velocity, nanofluid concentration, and the orientation of the fins, significantly influencing the heat recovery process. At an air velocity of 3 m/s, with 45° fin orientation and 0.15% by volume concentration of GO nanofluid, the Nusselt number and thermal performance factor increased by 60.01% and 41.92% respectively. It may be concluded that direct mounting of the finned circular tubes with proper orientation on the outer helical coiled surface plays a dual role in disturbing the flow and a potential waste heat tapping sources. Using nanofluid as a coolant in a closed loop further boosts the heat recovery process and the overall performance of the heat exchanger. While the present study focuses on only two fin orientations lot of scope exists for future research to optimize vital influencing parameters like cold fluid flow velocity, fin geometry, and the number of fins.

Compliance with ethical standards

Conflict of interest The authors declare that they have no conflict of interest.

Appendix A. Uncertainty calculations

A.1. Reynolds number

$$\frac{u\text{Re}}{\text{Re}} = \left[\left(\frac{u\rho}{\rho}\right)^2 + \left(\frac{uV}{V}\right)^2 + \left(\frac{ud_i}{d_i}\right)^2 + \left(\frac{u\mu}{\mu}\right)^2 \right]^{1/2}$$
$$= [(1 \times 10^{-5})^2 + (2.353 \times 10^{-3})^2 + (0.01)^2 + (9.980 \times 10^{-4})]^{1/2} = 0.0103$$

Hence uncertainty for Reynolds number is 1.03%

A.2. Heat gain

$$\frac{uQ}{Q} = \left[\left(\frac{um_c}{m_c}\right)^2 + \left(\frac{uC_p}{C_p}\right)^2 + \left(\frac{u\Delta T}{\Delta T}\right)^2 \right]^{1/2} = [(0.0299)^2 + (2.411 \times 10^{-4})^2 + (1.9531 \times 10^{-4}3)^2]^{1/2} = 0.0300$$

Hence uncertainty for Heat gain is 3.00%

A.3. Average heat transfer

$$uQ_{avg} = \left[\left(\frac{uQ_h}{Q_h} \right)^2 + \left(\frac{uQ_c}{Q_c} \right)^2 \right]^{1/2}$$

$$= \left[(0.0139)^2 + \left(2.6807 \times 10^{-3} \right)^2 \right]^{1/2} = 0.0141$$

Hence uncertainty for average heat transfer is 1.41%

A.4. Heat transfer coefficient

$$\frac{uh_i}{h_i} = \left[\left(\frac{uQ_{avg}}{Q_{avg}} \right)^2 + \left(\frac{u\Delta T}{\Delta T} \right)^2 + \left(\frac{uA}{A} \right)^2 \right]^{1/2}$$

$$= \left[(0.02308)^2 + \left(9.76 \times 10^{-4} \right)^2 + \left(0.01^2 \right) \right]^{1/2} = 0.0258$$

Hence uncertainty for heat transfer coefficient is 2.58%

A.5. Nusselt Number

$$\frac{uNu}{Nu} = \left[\left(\frac{uh}{h} \right)^2 + \left(\frac{ud_i}{d_i} \right)^2 + \left(\frac{uk}{k} \right)^2 \right]^{1/2}$$

$$= \left[\left(1.02711 \times 10^{-4} \right)^2 + (0.01)^2 + (0.016297^2) \right]^{1/2} = 0.0191$$

Hence uncertainty for Nusselt number is 1.91%

A.6. Friction factor

$$\frac{uf_c}{f_c} = \left[\left(\frac{u\mathrm{Re}}{\mathrm{Re}} \right)^2 + \left(\frac{ud_i}{d_i} \right)^2 + \left(\frac{uD_c}{D} \right)^2 \right]^{1/2}$$

$$= \left[\left(2.054 \times 10^{-5} \right)^2 + (0.01)^2 + \left(1.4285 \times 10^{-3} \right)^2 \right]^{1/2} = 0.0101$$

Hence uncertainty for friction factor is 1.01%

A.7. Thermal hydraulic performance

$$\frac{uT_{hp}}{T_{hp}} = \left[\left(\frac{uNu_w}{Nu_w} \right)^2 + \left(\frac{uNu_p}{Nu_p} \right)^2 + \left(\frac{uf c_w}{f c_w} \right)^2 + \left(\frac{uf c_p}{f c_p} \right)^2 + \left(\frac{u\delta}{\delta} \right)^2 \right]^{1/2}$$

$$= [(8.914 \times 10^{-3})^2 + (7070 \times 10^{-3})^2 + (3.92 \times 10^{-3})^2 + (1.77 \times 10^{-4})^2 + (7 \pm 10^{-5})]^{1/2} = 0.0118$$

Hence uncertainty for THP is 1.18%.

A.8. Overall uncertainty

$$u_{overall} = \left[\left(\frac{u_{\Delta T}}{\Delta T} \right)^2 + \left(\frac{u_m}{m} \right)^2 + \left(\frac{u_{\Delta p}}{\Delta p} \right)^2 + \left(\frac{u_W}{W} \right)^2 \right]^{1/2}$$

$$= [(9.7656 \times 10^{-6})^2 + (2.1417 \times 10^{-4})^2 + (0.02439)^2 + (2.5 \times 10^{-4})^2 + (7 \times 10^{-4})^2]^{1/2} = 0.0243$$

Hence overall uncertainty is 2.43%.

References

1. Kumar R, Chandra P (2020) Thermal analysis, pressure drop and exergy loss of energy efficient shell, and triple meshed helical coil tube heat exchanger. Energy Sources A Recovery Utilization Environ Effects 42(8):1026–1039
2. Gupta A, Kumar R, Gupta A (2014) Condensation of R-134a inside a helically coiled tube-in-shell heat exchanger. Exp Thermal Fluid Sci 54:279–289. https://doi.org/10.1016/j.expthermflusci.2014.01.003
3. Hardik BK, Baburajan PK, Prabhu SV (2015) Local heat transfer coefficient in helical coils with single phase flow. Int J Heat Mass Transf 89:522–538. https://doi.org/10.1016/j.ijheatmasstransfer.2015.05.069
4. Kumar A, Shukla SK (2019) Experimental and numerical analysis of a helical coil solar cavity receiver: thermal oil as the heat transfer fluid. Int J Green Energy 16:716–732. https://doi.org/10.1080/15435075.2019.1619566
5. Pawar SS, Sunnapwar VK, Tagalpallewar AR (2016) Development of experimental heat transfer correlations using Newtonian fluids in helical coils. Heat Mass Transf 52:169–181. https://doi.org/10.1007/s00231-015-1544-0
6. Lin CX, Ebadian MA (1997) Developing turbulent convective heat transfer in helical pipes. Int J Heat Mass Transf 40:3861–3873. https://doi.org/10.1016/S0017-9310(97)00042-2
7. Jayakumar JS, Mahajani SM, Mandal JC, Iyer KN, Vijayan PK (2010) CFD analysis of single-phase flows inside helically coiled tubes. Comput Chem Eng 34:430–446. https://doi.org/10.1016/j.compchemeng.2009.11.008
8. Babita SSK, Gupta SM (2019) Experimental studies on pressure drop and friction factor of CNT nanofluids flowing through helical coils and development of a new empirical correlation. J Dispersion Sci Technol 41:607–617. https://doi.org/10.1080/01932691.2019.1610420
9. Jamshidi N, Farhadi M, Ganji DD, Sedighi K (2013) Experimental analysis of heat transfer enhancement in shell and helical tube heat exchangers. Appl Therm Eng 51:644–652. https://doi.org/10.1016/j.applthermaleng.2012.10.008
10. Omidi M, Farhadi M, Ali A, Rabienataj D (2018) Numerical study of heat transfer on using lobed cross-sections in helical coil heat exchangers: effect of physical and geometrical parameters. Energy Conversion Manage 176:236–245. https://doi.org/10.1016/j.enconman.2018.09.034
11. Rakhsha M, Akbaridoust F, Abbassi A, Majid S (2015) Experimental and numerical investigations of turbulent forced convection flow of nanofluid in helical coiled tubes at constant

surface temperature. Powder Technol 283:178–189. https://doi.org/10.1016/j.powtec.2015.05.019

12. Ghorbani N, Taherian H, Mirgolbabaei H (2010) An experimental study of thermal performance of shell-and-coil heat exchangers. Int Commun Heat Mass Transf 37:775–781. https://doi.org/10.1016/j.icheatmasstransfer.2010.02.001

13. Akhavan-Behabadi MA, Pakdaman MF, Ghazvini M (2012) Experimental investigation on the convective heat transfer of nanofluid flow inside vertical helically coiled tubes under uniform wall temperature condition. Int Commun Heat Mass Transf 39:556–564. https://doi.org/10.1016/j.icheatmasstransfer.2012.02.008

14. Khosravi-Bizhaem H, Abbassi A (2018) Effects of curvature ratio on forced convection and entropy generation of nanofluid in a helical coil using two-phase approach. Adv Powder Technol 29:890–903. https://doi.org/10.1016/j.apt.2018.01.005

15. Boonsri R, Wongwises S (2015) Mathematical model for predicting the heat transfer characteristics of a helical-coiled, mathematical model for predicting a helical-coiled, crimped, spiral, finned -tube heat exchanger. Heat Transf Eng 36:1495–1503. https://doi.org/10.1080/01457632.2015.1024982

16. Sadeghzadeh HA, Aliehyaei M, Rosen MA (2015) Optimization of a finned shell and tube heat exchanger using a multi-objective optimization genetic algorithm. Sustainability 7:11679–11695. https://doi.org/10.3390/su70911679

17. Andrzejczyk R, Muszynski T, Gosz M (2018) Experimental investigations on heat transfer enhancement in shell coil heat exchanger with variable baffles geometry. Chem Eng Process Intensification 132:114–126. https://doi.org/10.1016/j.cep.2018.08.017

18. Nada SA, Khater R, Mahmoud MA (2020) Thermal characteristics enhancement of helical cooling-dehumidifying coils using strips fins. Therm Sci Eng Prog 45:631–647. https://doi.org/10.1016/j.tsep.2020.100482

19. Kumar RG, Chandra P (2018) Natural convection heat transfer from circular finned helical coil heat exchanger in eir. In: Bajpai PK, Panwar K (eds) Trends Manuf. Process ICFTMM2018, pp. 93–100. https://doi.org/10.1007/978-981-32-9099-0_10.

20. Hegde RN, Rao SS, Reddy RP (2012) Flow visualization and study of CHF enhancement in pool boiling with Al$_2$O$_3$ - water nanofluids. Therm Sci 16:445–453

21. Wang G, Yang J, Park J, Gou X, Wang B, Liu H, Yao J (2008) Facile synthesis and characterization of graphene nanosheets. J Phys Chem C 112:8192–8195

22. Hajjar Z, Rashidi A, Ghozatloo A (2014) Enhanced thermal conductivities of graphene oxide nanofluids. Int Commun Heat Mass Transf 57:128–131. https://doi.org/10.1016/j.icheatmasstransfer.2014.07.018

23. Stankovich S, Dikin DA., Piner RD, Kohlhaas KA, Kleinhammes A, Jia Y, Wu Y (2007) Synthesis of graphene-based nanosheets via chemical reduction of exfoliated graphite oxide. Carbon 45:1558–1565. https://doi.org/10.1016/j.carbon.2007.02.034

24. Holman JP (2012) Experimental methods for engineers, 8th edn. McGraw-Hill, New York

25. Fguiri A, Supérieur I, Marvillet C (2016) Design of a helical coil condenser of a small capacity water-lithium bromide absorption cooling machine. Int J Hydrogen Energy 42:8888–8897. https://doi.org/10.1016/j.ijhydene.2016.10.139

26. Seban RA, Mclaughlint EF (1963) Heat transfer in tube coils with laminar flow and turbulent flow. Int J Heat Mass Transf 6:387–395

27. Beigzadeh R, Rahimi M (2012) Prediction of heat transfer and flow characteristics in helically coiled tubes using artificial neural networks. Int Commun Heat Mass Transf 39:1279–1285. https://doi.org/10.1016/j.icheatmasstransfer.2012.06.008

28. Ijam A, Saidur R, Ganesan P, Golsheikh AM (2015) Stability, thermo-physical properties, and electrical conductivity of graphene oxide-deionized water-ethylene glycol-based nanofluid. Int J Heat Mass Transf 87:92–103. https://doi.org/10.1016/j.ijheatmasstransfer.2015.02.060

29. Kumar PC, Mukesh KJ, Suresh S (2013) Experimental investigation on convective heat transfer and friction factor in a helically coiled tube with Al$_2$O$_3$-water nanofluid. J Mech Sci Technol 27:239–245. https://doi.org/10.1007/s12206-012-1206-9

30. Sajid MU, Ali HM (2019) Recent advances in application of nanofluids in heat transfer devices: a critical review. Renew Sustain Energy Rev 103:556–592. https://doi.org/10.1016/j.rser.2018.12.057

31. Kannadasan N, Ramanathan K, Suresh S (2012) Comparison of heat transfer and pressure drop in horizontal and vertical helically coiled heat exchanger with CuO-water-based nanofluids. Exp Thermal Fluid Sci 42:64–70. https://doi.org/10.1016/j.expthermflusci.2012.03.031

32. Boles MA, Cengel YA (2013) Thermodynamics: an engineering approach (SI Units), 6th edn. Tata Mc.Graw-Hill Education, New York, pp 440–442.

33. Tan Y, He Z, Xu T, Fang X, Gao X (2017) Experimental investigation of heat transfer and pressure drop characteristics of non-Newtonian nanofluids flowing in the shell - side of a helical baffle heat exchanger with low-finned tubes. Heat Mass Transf 53:2813–2827. https://doi.org/10.1007/s00231-017-2015-6

34. Wang J, Saeed S, Alahgholi S, Mehri M, Safarzadeh M, Alimoradi A (2018) Analysis of exergy and energy in shell and helically coiled finned tube heat exchangers and design optimization. Int J Refrigeration 94:11–23. https://doi.org/10.1016/j.ijrefrig.2018.07.028

35. Naphon P (2007) Thermal performance and pressure drop of the helical-coil heat exchangers with and without helically crimped fins. Int Commun Heat Mass Transf 34:321–330. https://doi.org/10.1016/j.icheatmasstransfer.2006.11.009

Publisher's Note Springer Nature remains neutral with regard to jurisdictional claims in published maps and institutional affiliations.